Hyperspectral Analysis of Oil and Oil-Impacted Soils for Remote Sensing Purposes
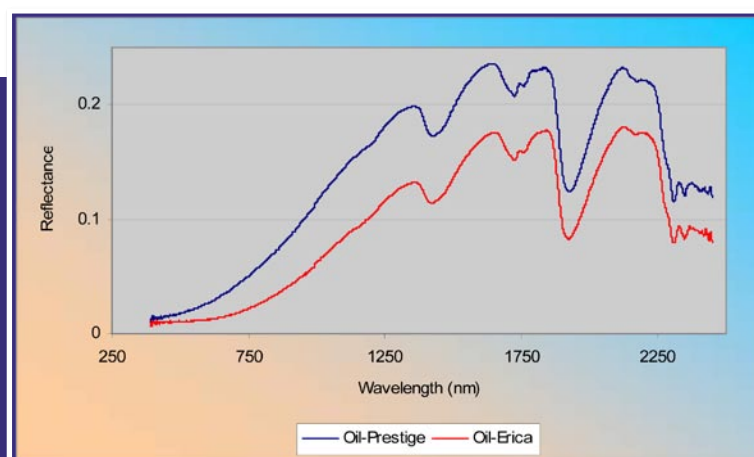
G.Andreoli, B.Bulgarelli, B.Hosgood, D.Tarchi

Institute for the Protection
and Security of the Citizen

Table of Contents

1. Introduction

Europe is the world's largest market in crude oil imports, representing about one third of the world total. Ninety percent of oil and refined products are transported to and from Europe by sea. Some of this oil makes its way into the sea - either due to accidental pollution, or deliberate oil discharge.

Oil spills ravage the fragile marine and coastal environments. They poison and suffocate countless aquatic creatures, like eider ducks, leatherback sea turtles, and polar bears. Immense tanker accidents discharge millions of liters of crude oil into the ocean. Yet, they represent only a small percentage of the tons of oil products discharged annually into our seas, mostly from smaller shipping operations, offshore rigs, and refineries. Other oil, leaked largely from automobiles, drains into storm sewers, waterways, and eventually oceans each year. Offshore oil spills hit hardest on coastal waters, the areas richest in biodiversity and the marine resources that humans depend on most. Oil, which is not evaporated or dispersed, tends to deposit on the seafloor or to hit the beaches, impacting the coastal ecology.

To lessen this impact, and create effective contingency planning, reliable monitoring methodologies and continuously updated comprehensive information are necessary.
Remote sensing represents a critical element for an effective response to marine oil spills: modern remote sensing instrumentation is a powerful tool both in preventing major disasters and in helping law enforcement for sea security.

A number of remote sensing systems are available for the detection and monitoring of oil slicks in the marine environment (Brekke and Solberg 2005, Fingas and Brown 1997). Conventional sensors are both passive (i.e., infrared cameras, optical sensors, infrared/ultraviolet systems, microwave radiometers) and active (i.e., laser fluorosensors and radar systems). Among them, the synthetic aperture radar (SAR) is still the most efficient and superior satellite sensor for operational oil spill detection, due to its wide area coverage and day and night all-weather capabilities. Nevertheless, it does not have capabilities for oil spill thickness estimation and oil type recognition, and it is only applicable for oil spill monitoring in a certain range of wind speeds. A part of the oil spill detection problem with SAR is to distinguishing oil slicks from other natural phenomena that dampen the short waves and create dark patches on the surface. These natural dark patches are termed oil slicks *look-alike*. A surprising number of false positive sightings may be seen. Ice, internal waves, kelp beds, natural organics, pollen, plankton blooms, cloud shadows, jellyfish, algae, guano washing off rocks, threshold wind speed areas (wind speed < 3m/s), wind sheltering by land, rain cells, and shear zones may all appear as oil (Espedal 1998).
It is the synergetic use of sensors working in different parts of the electromagnetic (EM) spectrum, which can achieve the most promising results.
Recently, hyperspectral sensors have started to be used for oil slick monitoring purposes.
While conventional multispectral sensors record the radiometric signal only at a handful of wavelengths, hyperspectral sensors measure the reflected solar signal at hundreds (100 to 200+) contiguous and narrow wavelength bands (bandwidth between 5 and 10 nm), spanning from the visible to the infrared. Hyperspectral images provide ample spectral information to identify and distinguish between spectrally similar (but unique) materials, providing the ability to make proper distinctions among materials with only subtle signature differences. Hyperspectral images show hence potentiality for proper discrimination between oil slicks and other natural phenomena (*look-alike*); and even for proper distinctions between oil types. Additionally they can give indications on oil volume.

At present, many airborne hyperspectral sensors are available to collect data, but only two civil spaceborn hyperspectral sensors exist as technology demonstrator: the Hyperion sensor on NASA's

EO-1 satellite and the CHRIS sensor on the European Space Agency's PROBA satellite. Consequently, the concrete opportunity to use spaceborn hyperspectral remote sensing for operational oil spill monitoring is yet not available. Nevertheless, it is clear that the future of satellite hyperspectral remote sensing of oil pollution in the marine/coastal environment is very promising.

In order to correctly interpret the hyperspectral data, the retrieved spectral signatures must be correlated to specific materials. Therefore specific spectral libraries, containing the spectral signature of the materials to be detected, must be built up. This requires that highly accurate reflected light measurements of samples of the investigated material must be performed in the lab or in the field.

Accurate measurements of the spectral reflectance of several samples of oil-contaminated soils have been performed in the laboratory, in the 400-2500 nm wavelength range. Samples of the oils spilt from the Erika and the Prestige tankers during the major accidents of 1999 and 2002 were also collected and analyzed in the same spectral range, using a portable spectrophotometer. All measurements showed the typical absorption features of hydrocarbon-bearing substances: the two absorption peaks centered at 1732 and 2310 nm. This is in perfect agreement with the findings of E. Cloutis (1989).
The above measurements allow the building up of an oil-focused spectral library, which includes the spectral signatures of pure oil and oil-impacted soils and which will make the detection process of oil-slicks more rapid and reliable.

In Section 2 a general description of a hyperspectral sensor is given. Section 3 gives an overview of the algorithms and methodologies used for the interpretation of remotely sensed hyperspectral data, and which are of interest for oil spill monitoring. Recent applications of hyperspectral remote sensing to the monitoring of hydrocarbons in the marine/coastal environment are presented in Section 4. The hyperspectral measurements performed *in situ* and in the laboratory are described in Section 5.

2. Hyperspectral sensors

Hyperspectral remote sensing, also known as imaging spectroscopy, is a relatively new technology that is currently being investigated by researchers and scientists with regard to the detection and identification of minerals, terrestrial vegetation, and man-made materials and backgrounds and to monitor land, water and atmosphere.

Imaging spectroscopy has been used in the laboratory by physicists and chemists for over 100 years for identification of materials and their composition. Spectroscopy can be used to detect individual absorption features due to specific chemical bonds in a solid, liquid, or gas. Recently, with advancing technology, imaging spectroscopy has begun to focus on the Earth. The concept of hyperspectral remote sensing began in the mid-80's and to this point has been used most widely by geologists for the mapping of minerals. Actual detection of materials is dependent on the spectral coverage, spectral resolution, and signal-to-noise of the spectrometer, the abundance of the material and the strength of absorption features for that material in the wavelength region measured.

Hyperspectral remote sensing combines imaging and spectroscopy in a single system which often includes large data sets and requires new processing methods.

2.1 The spectral signature

Any given material will reflect, absorb or transmit the electromagnetic (EM) radiation at different wavelengths in a unique and specific way. The specific combination of reflected and absorbed EM radiation at varying wavelengths is called the "spectral signature".

As an example, Figure 1 shows the reflectance spectra (i.e., the percentage of reflected EM radiation) measured by laboratory spectrometers for three materials: a green bay laurel leaf, the mineral talc and a silty loam soil. Field and laboratory spectrometers usually measure reflectance at many narrow, closely spaced wavelength bands, so that the resulting spectra appear to be continuous curves.
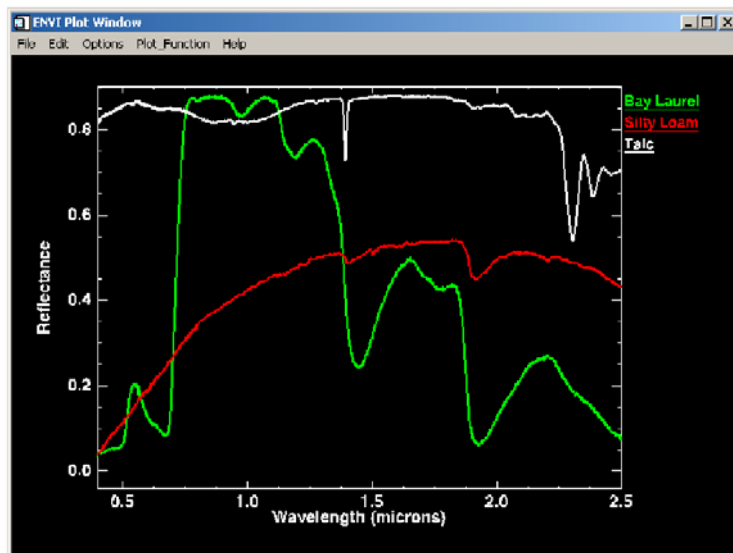
Figure 1. Spectral signature (percentage of reflected EM radiation versus wavelength) measured by laboratory spectrometers for three materials: a green bay laurel leaf, the mineral talc and a silty loam soil. (source: Shippert 2004)

2.2. Hyperspectral Data

Like the laboratory spectroradiometers, hyperspectral sensors can record about 100 to 200+ contiguous selected wavelengths of reflected and emitted energy, with high spectral resolution (5-10 nm), enabling the construction of an effective, and continuous reflectance spectrum for every pixel scene (Figure 2 and 3).
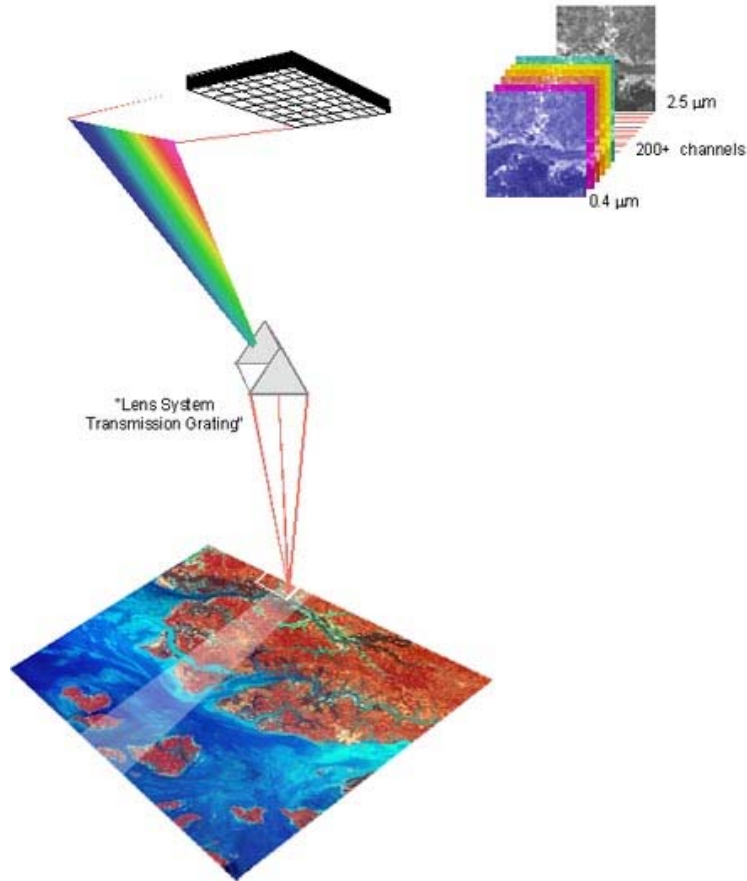
Figure 2. Hyperspectral Imaging (source: Canadian Space Agency)
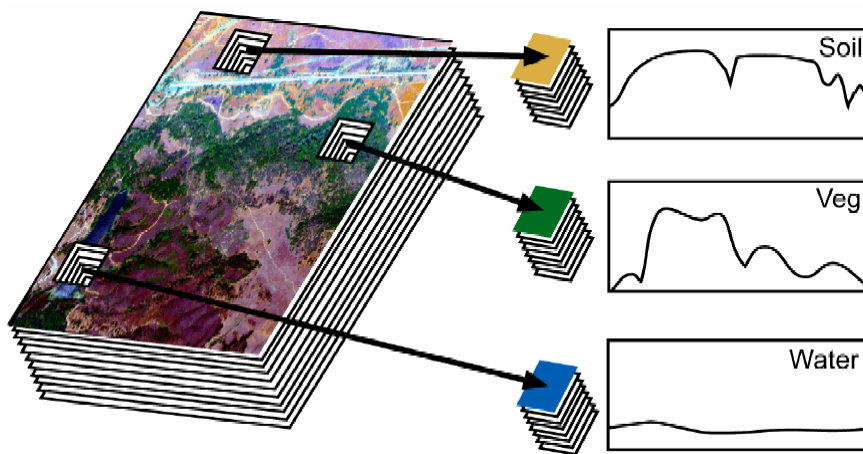
Figure 3. The concept of hyperspectral imagery. (source: Shippert 2004)

The electromagnetic spectrum covered by a range of hyperspectral imagers is shown in Figure 4.
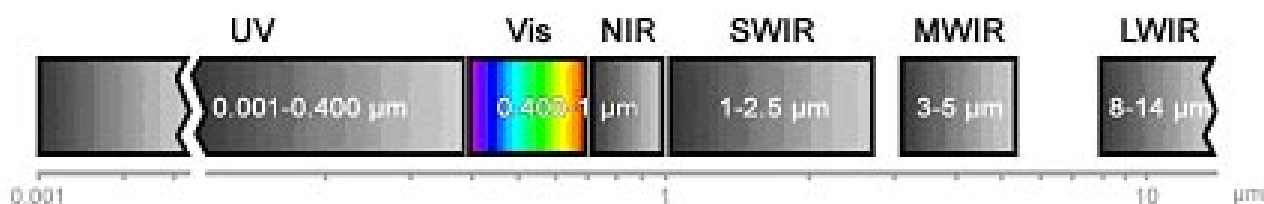
Figure 4: Typical Hyperspectral Frequency Bands (Vis Visible; NIR Near infrared; SWIR Short wavelength infrared; MWIR Medium wavelength infrared ; LWIR Long wavelength infrared)

With respect to conventional multispectral sensors, which record the target radiance only at a handful of wavelengths with broad bandwidth (20-400 nm), hyperspectral data sets allow an almost complete reconstruction of the spectral signature: the retrieved spectrum for each pixel appears very much like the spectrum that would be measured in a spectroscopy laboratory. This is well illustrated in Figure 5, which depicts the reflectance spectra of the three materials of Figure 1 as they would appear to the multispectral Landsat 7 ETM sensor and to the hyperspectral AVIRIS sensor. The gaps in the spectra belong to wavelength ranges at which the atmospheric transmittance is so low that no reliable signal is received from the surface.

It is important to underline that, although most hyperspectral sensors measure hundreds of wavelengths, it is not the number of measured wavelengths that defines a sensor as hyperspectral. Rather it is the narrowness and contiguous nature of the measurements.

Hyperspectral imagery provides an opportunity for more detailed image analysis. Using hyperspectral data, spectrally similar (but unique) materials can be identified and distinguished, and sub-pixel scale information can be extracted.

Table 1 lists the principal applications which can take advantages from hyperspectral remote sensing.

Table 1. Principal applications which can take advantage of hyperspectral remote sensing

|	
Atmosphere	water vapor, cloud properties, aerosols
Ecology	chlorophyll, leaf water, cellulose, pigments, lignin
Geology	mineral and soil types
Coastal Waters	chlorophyll, phytoplankton, dissolved organic materials, suspended sediments
Snow/Ice	snow cover fraction, grainsize, melting
Biomass Burning	subpixel temperatures, smoke
Commercial	mineral (oil) exploration, agriculture and forest production
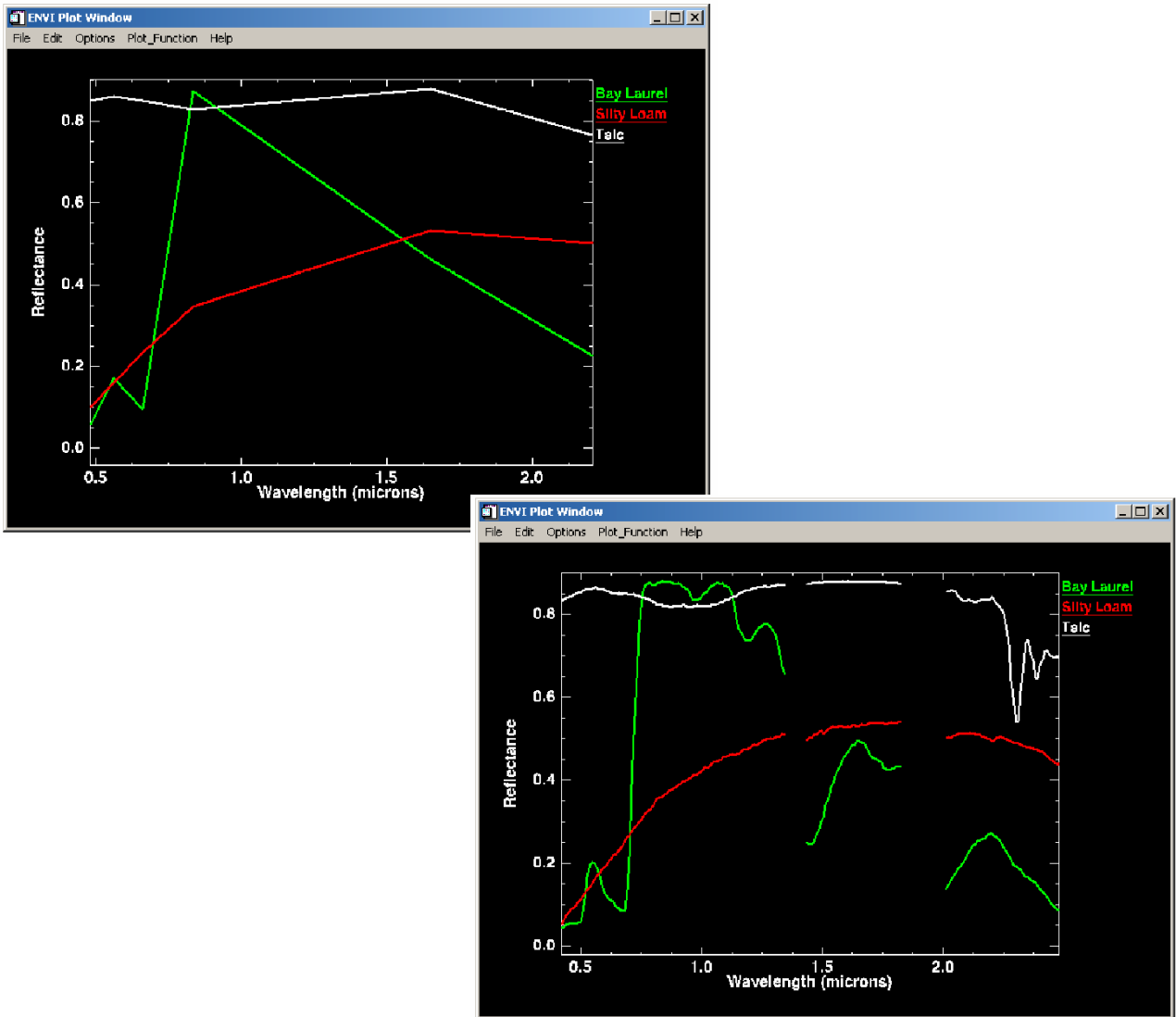
Figure 5: reflectance spectra of the three materials in Figure 1; on the left: as they would appear to the multispectral Landsat 7 ETM sensor; on the right: as they would appear to the hyperspectral AVIRIS sensor. The gaps in the spectra are wavelength ranges at which the atmosphere absorbs so much light that no reliable signal is received from the surface (source: Shippert 2004)

8

2.3 Hyperspectral versus radar sensors

The SAR is still the most efficient and superior satellite sensor for operational oil spill detection in the marine environment. SAR detects oil features floating on the surface, exploiting the property of oil to dampen the Bragg waves (wavelength of a few cm) on the ocean surface, which leads to a decreased backscattered signal. SAR is particularly useful for observing ocean at night and in cloudy weather conditions, thanks to its all-day and all-weather capabilities.

Hyperspectral sensors do not work at night and in cloudy conditions, but with respect to radar sensors, they consent to measure an intrinsic property of the observed feature: its spectral signature. Consequently, these sensors afford the potential for detailed identification of materials (eliminating the false alarm features) and better estimate of their abundance. In other words, distinction between man-made oil slicks and natural slicks, oil type classification (light/crude oil), and estimate of oil spill thickness (i.e., its volume) should be feasible. Moreover, since the light penetrates through the water surface, when monitoring oil spills in the marine environment, hyperspectral (but also multispectral) sensors can potentially detect submerged oil slicks and dispersed oil droplets (emulsion). Hyperspectral sensors offer also the potentiality to detect oil-impacted soils as a consequence of oil-beaching, occurred, for example, as a consequence of the Prestige and Erika accidents and of the Lebanon Jieh power plant bombing.

2.4 Recent and current hyperspectral sensors

Most past and current hyperspectral sensors have been airborne (Table 2), with three recent exceptions: the U.S. Air Force Research Lab's FTHSI sensor on the MightySat II satellite, the NASA's Hyperion sensor on the EO-1 satellite, and the ESA's CHRIS sensor on the PROBA satellite. All of them are non-commercial space-borne technology demonstrators. Several new space-based hyperspectral sensors have been proposed recently. Unlike airborne sensors, space-based sensors are able to provide near global coverage repeated at regular intervals. Therefore, the amount of hyperspectral imagery available should increase significantly in the near future as new satellite-based sensors are successfully launched.

FTHSI

MightySat II.1 is a technology demonstration mission of the US Defense Space Test Program (test of high-risk, high-payoff space system technologies). The MightySat II program, initiated in March 1996, represents a series of up to five small satellite missions over a decade. The Fourier Transform HyperSpectral Imager (FTHSI) was designed and built by Kestrel Corporation of Albuquerque, NM, and the Florida Institute of Technology, Melbourne, FL, heritage of airborne version of FTVHSI. The objective was to demonstrate spaceborne hyperspectral imaging technologies. This instrument has been the first earth remote-sensing hyperspectral imager collecting data from space, and produced valuable data from shortly after launch (July 2000) until it was turned off in October 2001. The nominal Ground Sampling Distance (GSD) is 30 m.

Hyperion

The Hyperion Imaging Spectrometer is a hyperspectral sensor which collects 220 unique spectral channels ranging from 0.357 to 2.576 micrometers with a 10-nm bandwidth. It is a pushbroom instrument. Each image frame taken in this configuration captures the spectrum of a line 30 m long by 7.5 km wide, perpendicular to the satellite motion. Standard scene length is 42 kilometers, with an optional increased scene length of 185 kilometers.

Hyperion flies on board the Earth Observing-1 (EO-1) NASA satellite, launched on November 21, 2000 as part of a one-year technology validation/demonstration mission. The original EO-1 Mission was successfully completed in November 2001. Based on the interest of the remote sensing research and scientific communities, an agreement was reached between NASA and the United States

Geological Survey to allow continuation of the EO-1 Program as an Extended Mission. The EO-1 Extended Mission is chartered to collect and distribute ALI (Advanced Land Imager) multispectral and Hyperion hyperspectral products in response to Data Acquisition Requests (DARs). Under the Extended Mission provisions, image data acquired by EO-1 are archived and distributed by the USGS Center for Earth Resources Observation and Science (EROS) and placed in the public domain (http://edc.usgs.gov/products/satellite/eo1.html).

The EO-1 satellite follows a repetitive, circular, sun-synchronous, near-polar orbit with a nominal altitude of 705 km at the Equator. The spacecraft travels from north to south on the descending (daytime) orbital node, maintaining a mean equatorial crossing time between 10:00 AM and 10:15 AM for each daytime pass. The satellite circles the Earth at 7.5 km/sec, with an orbit inclination of 98.2 degrees and an orbital period of 98.9 minutes. Each orbit takes nearly 99 minutes, and the velocity of the EO-1 nadir point is 6.74 km/sec. EO-1 completes just over 14 orbits per day, with a repeat cycle of 16 days.

EO-1 follows the same orbit as Landsat 7, trailing the latter by one minute (+/- five seconds). This orbit has been very useful for obtaining cross comparisons of instrument performance from the two satellites. Because EO-1 is much smaller and lighter than Landsat 7, periodic burns are required in order to maintain this distance, thus preventing EO-1 from overtaking Landsat 7.

CHRIS

The CHRIS (Compact High Resolution Imaging Spectrometer) is an imaging spectrometer, carried on board the ESA space platform called PROBA (Project for On Board Autonomy), successfully launched on October 22, 2001.

The instruments on board are CHRIS, DEBIE (Debris In-Orbit Evaluator) and SREM (Standard Radiation Environment Monitor). PROBA also carries two imagers, a Wide Angle Camera (WAC) and a High Resolution Camera (HRC) with a 10 metre resolution.

CHRIS is an AO hyperspectral instrument whose objective is the collection of BRDF (Bidirectional Reflectance Distribution Function) data for a better understanding of spectral reflectances. CHRIS provides 19 spectral bands (fully programmable) in the VNIR range (400 - 1050 nm) at a GSD of 17 m. Each nominal image forms a square of 13 km x 13 km on the ground (at perigee). The observation of the square target area consists in 5 consecutive pushbroom scans by the single-line array detectors. CHRIS can be reconfigured to provide 63 spectral bands at a spatial resolution of about 34 m. The CHRIS design is capable of providing up to 150 channels over the spectral range of 400-1050 nm. The repeat cycle is approximately 7 days.

Table 2. Selected Recent and Current Satellite and Airborne Hyperspectral Sensors

Satellite Sensor	Organization	Number of Bands	Wavelength Range (nm)
Hyperion on EO-1	NASA Goddard Space Flight Center http://www.gsfc.nasa.gov	220	400-2.500
CHRIS (Compact High Resolution Imaging Spectrometer) on PROBA	European Space Agency http://www.esa.int	150	450-1.050
FTHSI (Fourier-Transform Visible Hyperspectral Imager) on MightySat II NOW OFF	Operated by Air Force Research Labs http://www.vs.afrl.af.mil/TechProgs/MightySatII designed by Kestrel Corp. http://www.kestrelcorp.com/	256	350-1.050
Airborne Sensor	**Organization**	**Number of Bands**	**Wavelength Range (nm)**
AHS (Airborne Hyperspectral Scanner)	SenSyTech http://www.sensytech.com	48	433-12.700
AISA (Airborne Imaging Spectrometer for Applications)	Spectral Imaging http://www.specim.fi	Up to 288	430-1.000
AVIRIS (Airborne Visible/Infrared Imaging Spectrometer)	NASA Jet Propulsion Lab http://www.makalu.jpl.nasa.gov/	224	400-2.500
CASI (Compact Airborne Spectrographic Imager)	ITRES Research Limited http://www.itres.com	Up to 228	400-1.000
DAIS 7915 (Digital Airborne Imaging Spectrometer)	GER Corp. http://www.ger.com	79	430-12.300
EPS-H (Environmental Protection System)	GER Corp. http://www.ger.com	152	430-12.500
HYDICE (Hyperspectral Digital Imagery Collection Experiment)	Naval Research Lab	210	400 – 2.500
HyMap	Integrated Spectronics http://www.intspec.com	100 to 200	Visible to thermal infrared
MIVIS (Multispectral Infrared and Visible Imaging Spectrometer)	SenSyTech http://www.sensytech.com	102	400-2.500
PROBE-1	Earth Search Sciences Inc. http://www.earthsearch.com	128	400-2.500
SFSI (Short Wavelength Infrared Full Spectrum Imager)	Canadian Centre for Remote Sensing http://www.ccrs.nrcan.gc.ca/ccrs/tekrd/rd/acc/sfsi/sfsie.html	120	1,200-2,400
TRWIS III (TRW Imaging Spectrometer)	TRW Inc. http://www.trw.com	384	380-2,450

* Indicates satellite-based sensor. All other hyperspectral sensors listed are airborne.

11

3. Hyperspectral image analysis: an overview

There are four main oil characteristics that should be remotely retrieved for operational purposes: oil slick position, global volume of the oil contained in the slick, oil type and forecast of the drift trajectory.

Hyperspectral sensors have the potential to detect the slick position, to retrieve information on the nature of the slick, to give indications on oil type (crude/light) and thickness, to detect submerged oil slicks, emulsions and oil-impacted soils as a consequence of beaching.

Standard multispectral image classification techniques were generally developed to classify multispectral images into broad categories. To fulfill the new potential of hyperspectral data, new image processing techniques have been developed. Different retrieval algorithms are applied when focusing on specific EM regions (i.e., VIS, NIR and SWIR) or when considering the whole spectrum at once. Particularly interesting for the application of hyperspectral remote sensing to oil pollution monitoring are algorithms and methodologies developed in geological remote sensing, more specifically in the field of oil seep (macro- and micro-seepages) monitoring.

In this section an overview of the principal algorithms and methodologies for hyperspectral data analysis will be given. The overview is not intended to be exhaustive, but its scope is to illustrate some procedures which can be applied for hyperspectral oil spill monitoring purposes.

3.1 Analysis of the contrast in the SWIR

As found by Cloutis in 1989 and as presented in Section 5, hydrocarbon-bearing substances show characteristics absorption peaks at 1730 and 2310 nm, i.e., in the SWIR. Focusing hyperspectral remote sensing observation on this region, hydrocarbon can be detected efficiently and unambiguously. The above findings have been already used for the detection of oil contaminated areas by Kuehn and Hoerig (1995).

Hoerig et al. (2001) showed that the same hydrocarbons spectral maxima/minima characteristics measured *in situ*, could be seen by a HyMap sensors flying on board an airplane. The absorption peaks (or radiance minimum) could be recognized in the HyMap pixel spectra, despite noise produced by the atmosphere between the scanner and the ground. Although less prominent, the peaks were still significant enough for hydrocarbon-bearing materials to be detected when the pixel spectra were evaluated. However, efficient mapping of the locations of hydrocarbons required image processing capable of accentuating all pixels with such absorption maxima. Following the above considerations, the same authors (Kuehn et al. 2004) developed a Hydrocarbon Index (HI) focused on the 1730 nm absorption peak (Eq. 1 and Fig. 6):

$$HI = (\lambda_B - \lambda_A) \frac{R_C - R_A}{\lambda_C - \lambda_A} + R_A - R_B \tag{1}$$

where, for the HyMap sensor: λ_A=1705 nm; λ_B=1729 nm and λ_C=1741 nm; while R_A, R_B and R_C are the correspondent radiance values. Other wavelengths may be necessary for other scanners. If hydrocarbon-bearing material is present at the surface, HI>0. If no hydrocarbon-bearing material is present, HI=0. It is worthwhile to underline that the HI has been developed for the detection of oil-impacted soils and that the absorption peak at 1730 nm is very closed to a strong water absorption band.
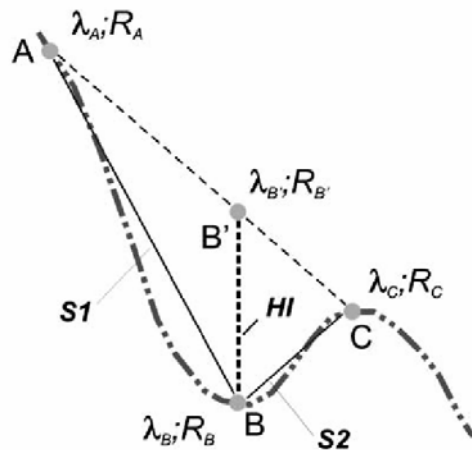
Figure 6. Enlarged 1730 nm portion of the spectral signature (radiance) of hydrocarbon-bearing materials with 'index points' A, B, B' and C for the Hydrocarbon Index; R_i and λ_i are the radiance values and wavelengths at the 'index points' (source Kuehn et al., 2004)

An analogous algorithm for the 2310 nm absorption feature is described in the NASA "Remote Sensing Tutorial" (NASA, 2006): a ratio of two reflectance values on either side of that absorption feature divided by the value of the decreased reflectance in the spectral curve at the feature low point enhances the detectability of the hydrocarbon and quantifies its magnitude (Figure 7).

Figure 7. Hydrocarbon Detection Index (source NASA, 2006)

13

Hoerig et al. (2001) demonstrated that, at least for airborne remote sensing of oil-contaminated soil, if the image processing is focused on the hydrocarbon spectral characteristics, atmospheric corrections of the data are not necessary.
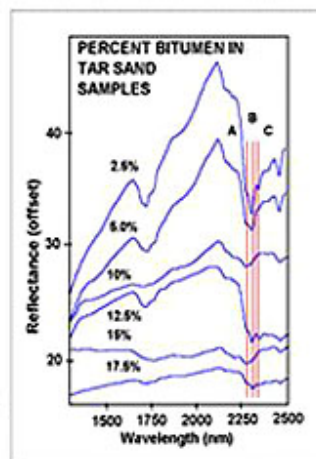
Both algorithms described above are sensitive to the amount of hydrocarbon. The deeper the minimum, the higher is the oil amount. As an approximation, it can be assumed that the larger the index value, the larger the hydrocarbon concentration. Nevertheless the estimate of oil abundance is only qualitative and not quantitative.

3.2 Analysis of the contrast in the VIS/NIR

Recently, it has been shown that the medium-resolution multispectral sensor MODIS (with a spatial resolution up to ~250m), provides direct potentiality for large oil spill detection in water basins (Hu et al. 2003, Bulgarelli and Tarchi, 2006).

In comparison with seawater, oil is characterized by higher refractive index and absorption (Byfeld and Boxal, 1999). Hence, when oil is floating on the sea surface, the reflected signal increases while the signal leaving the water body (the so called *water leaving radiance*) decreases. As a net effect, an optical contrast between oil and surrounding seawater appears. Radiative transfer simulations (Otremba and Piskozub, 2001, 2002, 2004) show that, while the optical contrast of oil droplets dispersed in the water (emulsions) is always positive, that of an oil slick floating on the sea surface can range from positive to negative depending on several different parameters: oil type, oil thickness, illumination and observation geometry, optical properties of the water body, sea surface state (wind, sea surface roughness).

The above considerations mean that VIS/NIR contrast analysis allows detecting the oil slick position, and that, in principle, there is also the potential to retrieve oil thickness indications, once all other relevant parameters are known. Any image-enhancing software can be used to contrast-stretch an image and help identify and trace the oil slick; nevertheless only proper atmospheric correction provides meaningful geophysical data, offering the potential to derive additional indications (i.e., oil film thickness). It is therefore underlined that the retrieval of oil spill information from VIS/NIR requires a highly accurate, validated and operational atmospheric correction procedure.

3.3 Retrieval of the spectral signature

A full exploitation of hyperspectral data is only obtained when retrieving the whole spectral signature of the substance to be detected, from VIS to SWIR.

Hyperspectral images are sometimes referred to as "image cubes" because they have a large spectral dimension as well as the two spatial dimensions (Figure 8). Hyperspectral data (or spectra) can be thought of as points in an *n*-dimensional scatterplot. The data for a given pixel corresponds to a spectral reflectance for that given pixel. The distribution of the hyperspectral data in *n*-space can be used to estimate the number of spectral endmembers (i.e., the set of spectrally unique surface materials existing within a scene) and their pure spectral signatures and to help understand the spectral characteristics of the materials which make up that signature. Typically, the analysis of a hyperspectral scene involves the decomposition of each pixel in the image into its constituents, where these are represented by spectra of relatively pure material, which are themselves extracted from the scene. The identity of these constituents is determined by comparison with 'library' spectra of known materials measured in the field or in the laboratory.
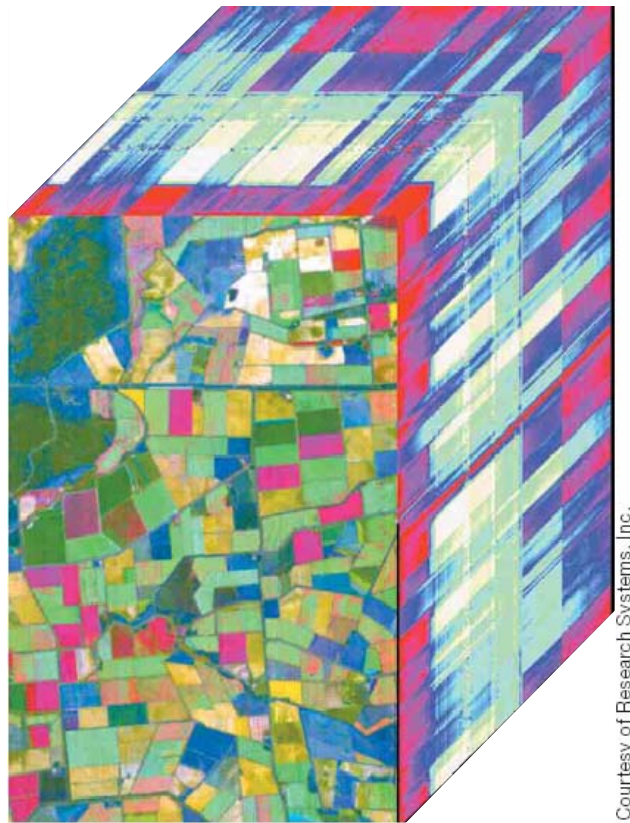
Figure 8. Hyperspectral images are sometimes referred to as "image cubes" because of the large number of measured wavelengths. The face of the cube in this example is an image of an agricultural region in Australia, which was collected by the Hyperion sensor. The top and right side of the cube show hundreds of color-coded pixel values measured for each pixel along the top and right edge of the image.

A short recall of the new hyperspectral image processing techniques (source: Shippert 2004) is given here for completeness.

Boardman (1993) and Boardman et al. (1995) were among the first to develop and commercialize a sequence of algorithms specifically designed to extract detailed information from hyperspectral imagery. These tools, applicable to a variety of applications, distinguish and identify the unique materials present in the scene and map them throughout the image. They remain the most widely used image analysis tools for working with hyperspectral imagery. Tetracorder has been used to identify and map surface minerals, water, snow, vegetation, pollution, human-made objects and other phenomena through the analysis of hyperspectral data (Clark et al., 2003). Another algorithm for identifying the unique materials within a hyperspectral scene, known as Sequential Maximum Angle Convex Cone (SMACC), has recently been developed by Spectral Sciences Inc. (Gruninger et al. 2001) to be included in commercial softwares. Most commercial image processing software packages now include tools for analyzing hyperspectral imagery. These tools are being continually refined, expanded and simplified.

The standard procedure to interpret hyperspectral data includes: *i)* the performance of the atmospheric correction; *ii)* the identification of target; and *iii)* its classification, usually with the use of spectral libraries.

3.3.1 Atmospheric correction
Quantitative information extraction usually requires accurate preprocessing of the hyperspectral imagery and collection of accurate auxiliary data. Among the first challenges faced when performing quantitative analysis of hyperspectral data are those encountered due to the atmosphere.

The solar radiation while traveling from the sun to the target and from the target to the sensor interacts with the atmosphere, through absorption and diffusion processes. Hence, data collected by the satellites are largely contaminated by atmospheric effects. The objective of atmospheric correction is to retrieve the surface reflectance (that characterizes the surface properties) from remotely sensed imagery by removing these atmospheric effects.

A variety of atmospheric correction algorithms have been developed for the processing of hyperspectral data, among them: the ENVI atmospheric correction module FLAASH (Fast Line-of-sight Atmosphere Analysis of Spectral Hypercubes; Matthew et al., 2000); a series of Atmospheric and Topographic CORrection codes (ATCOR) (Richter 1997); the Atmosphere CORrection Now algorithm (ACORN; Green 2001), the High-accuracy Atmospheric Correction for Hyperspectral data (HATCH; Qu et al. 2003); and the ATmosphere REMoval Algorithm (ATREM; Gao et el. 1996). All these algorithms are mostly designed for remote sensing of land surfaces. Since the signal leaving the water is much lower than that of land and the air/water interface is not Lambertian, problems can occur when the above algorithms are applied in the correction of marine pixels. Specific research has been done for removing the atmospheric effects from hyperspectral marine and coastal data. The TAAFKA atmospheric correction module has been, for example, expressly developed for hyperspectral ocean color images (Gao et al. 2000).

3.3.2 Spectral libraries
Spectral libraries are collections of reflectance spectra measured from materials of known composition. They require that highly accurate reflected light measurements of samples of the investigated material are performed in the lab or in the field (as shown in Section 5). In the present specific case, an oil dedicated spectral library is needed.

3.3.3 Target identification and classification: unmixing and subpixel algorithms
There are many unique image analysis algorithms that have been developed to exploit the extensive information contained in hyperspectral imagery. Spectral analysis methods usually compare pixel spectra with a reference spectrum (often called a *target*). Target spectra can be derived not only from spectral libraries, but also from regions of interest within a spectral image, or individual pixels within a spectral image.

Some commonly used hyperspectral image analysis methods (also provided by ENVI) are described below.

Whole Pixel Methods
Whole pixel analysis methods attempt to determine whether one or more target materials are abundant within each pixel in a multispectral or hyperspectral image on the basis of the spectral similarity between the pixel and target spectra. Whole-pixel scale tools include standard supervised classifiers such as Minimum Distance or Maximum Likelihood (Richards and Jia, 2006), as well as tools developed specifically for hyperspectral imagery such as, for example, Spectral Angle Mapper, Spectral Feature Fitting, Derivative Spectroscopy.

Spectral Angle Mapper (SAM)

In a scatter plot of pixel values from two bands of a spectral image, pixel spectra and target spectra will plot as points (Fig. 9). If a vector is drawn from the origin through each point, the angle between any two vectors constitutes the spectral angle between those two points. The Spectral Angle Mapper (Kruse et al., 1993) computes a spectral angle between each pixel spectrum and each target spectrum. The smaller the spectral angle, the more similar the pixel and target spectra. This spectral angle will be relatively insensitive to changes in pixel illumination because increasing or decreasing illumination doesn't change the direction of the vector, only its magnitude (i.e., a darker pixel will plot along the same vector, but closer to the origin). Clearly, although this discussion describes the calculated spectral angle using a two-dimensional scatter plot, the actual spectral angle calculation is based on all of the bands in the image. In the case of a hyperspectral image, a spectral "hyper-angle" is calculated between each pixel and each target.
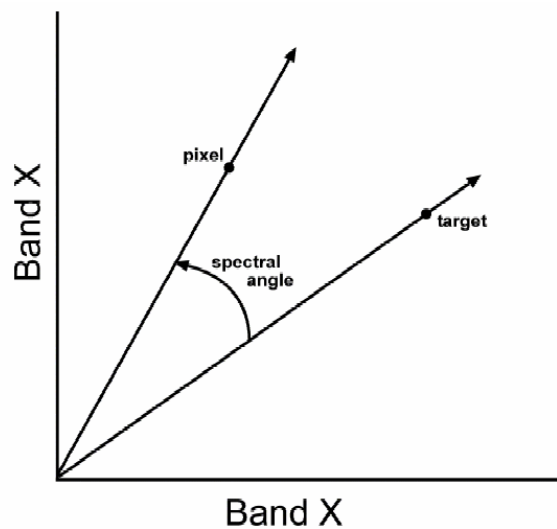

Figure 9. The Spectral Angle Mapper concept.

Another approach to matching target and pixel spectra is by examining specific absorption features in the spectra:

Spectral Feature Fitting

The Spectral Feature Fitting allows the user to specify a range of wavelengths within which a unique absorption feature exists for the chosen target. The pixel spectra are then compared to the target spectrum using two measurements: 1) the depth of the feature in the pixel is compared to the depth of the feature in the target, and 2) the shape of the feature in the pixel is compared to the shape of the feature in the target (using a least-squares technique). Spectral Feature Fitting is a relatively simple form (available in ENVI) of the Tetracorder method (Clark et al., 2003).

Derivative Spectroscopy

Derivative Spectroscopy analysis of hyperspectral data provides a method for quickly identifying spectral absorption features, thereby simplifying large numerical data sets into smaller, manageable units. The enhancement of absorption features is done using finite approximation to calculate the change in reflectance over a bandwidth $\Delta\lambda$ defined as $\Delta\lambda=\lambda_j-\lambda_I$, where $\lambda_j>\lambda_i$ (Tsai and Philpot, 1998). The estimation of the *n*th derivative calculated as (Eq. 2):

$$\left. \frac{d^n s}{d\lambda^n} \right|_j = \frac{d}{d\lambda}\left(\frac{d^{(n-1)}s}{d\lambda^{(n-1)}} \right) \tag{2}$$

Derivative spectroscopy is a powerful tool that is commonly used in the analysis of hyperspectral remote sensing data from terrestrial environment. It is able to enhance minute fluctuations in reflectance spectral and separate closely related absorption features. A primary application has been to analyze pigment and chemical composition of leaves in order to track physiological changes in plant canopies.

Sub-Pixel Methods
Sub-pixel analysis methods can be used to calculate the quantity of target materials in each pixel of an image. Sub-pixel analysis can detect quantities of a target that are much smaller than the pixel size itself. In cases of good spectral contrast between a target and its background, sub-pixel analysis has detected targets covering as little as 1-3% of the pixel. Sub-pixel analysis methods include Complete Linear Spectral Unmixing, and Matched Filtering.

 Complete Linear Spectral Unmixing
The set of spectrally unique surface materials existing within a scene are often referred to as the spectral endmembers for that scene. Linear Spectral Unmixing (Adams et al., 1986; Boardman, 1989) exploits the theory that the reflectance spectrum of any pixel is the result of linear combinations of the spectra of all endmembers inside that pixel. A linear combination in this context can be thought of as a weighted average, where each endmember weight is directly proportional to the area the pixel containing that endmember. If the spectra of all endmembers in the scene are known, then their abundances within each pixel can be calculated from each pixel's spectrum. Unmixing simply solves a set of *n* linear equations for each pixel, where *n* is the number of bands in the image. The unknown variables in these equations are the fractions of each endmember in the pixel. To be able to solve the linear equations for the unknown pixel fractions it is necessary to have more equations than unknowns, i.e., more bands than endmember materials. With hyperspectral data this is almost always true. The results of Linear Spectral Unmixing include one abundance image for each endmember. The pixel values in these images indicate the percentage of the pixel made up of that endmember. An error image is also usually calculated to help evaluate the success of the unmixing analysis.

 Matched Filtering
Matched Filtering (Boardman et al., 1995) is a type of unmixing in which only user-chosen targets are mapped. Unlike Complete Unmixing, there is no need to find the spectra of all endmembers in the scene to get an accurate analysis (hence, this type of analysis is often called a 'partial unmixing' because the unmixing equations are only partially solved). Matched Filtering was originally developed to compute abundances of targets that are relatively rare in the scene. If the target is not rare, special care must be taken when applying and interpreting Matched Filtering results. Matched Filtering "filters" the input image for good matches to the chosen target spectrum by maximizing the response of the target spectrum within the data and suppressing the response of everything else (which is treated as a composite unknown background to the target). Like Complete Unmixing, a pixel value in the output image is proportional to the fraction of the pixel that contains the target material. Any pixel with a value of 0 or less would be interpreted as background (i.e., none of the target is present). One potential problem with Matched Filtering is that it is possible to end up with false positive results.

4. Recent hyperspectral applications for oil spill detection in the marine/coastal environment and further considerations

Crude oil seeps naturally from geologic strata beneath the seafloor into water. They contribute the highest amount of oil to the marine environment, accounting for 46 per cent of the annual load to the world's oceans (NRC 2003). Natural oil seeps are commonly used in identifying potential petroleum reserves. Although entirely natural, these seeps significantly alter the nature of nearby marine environments; hence, they serve as natural laboratories where researchers can learn how marine organisms adapt over generations of chemical exposure. Seeps illustrate how dramatically animal and plant population levels can change with exposure to ocean petroleum.

In early 2000 a cooperative R&D project, sponsored by Chevron, ExxonMobil and Royal Dutch/Shell, was initiated by the HJW Geospatial Inc. and the Geosat Committee Inc. to determine the viability of hyperspectral technology for detecting oil seeps and oil-impacted soils. The Geosat project proved that sophisticated airborne hyperspectral sensors were capable of detecting oil seeps and oil-impacted soils (Ellis 2001, Ellis 2003). The ENVI Software was used to extract subtle hydrocarbon signature from airborne hyperspectral datacubes. The research project demonstrated that facility managers, engineers, environmental scientists and geologists could use these technologies to obtain traditional maps and to detect oil-impacted sites, subtle variation in vegetation vigor, different plant types and differences among disturbed and engineered soils.

Hyperspectral imagery is now regularly used by the private sector for oil exploration purpose (e.g.:Ellis GeoSpatial www.ellis-geospatial.com; Earth SearchSciences Inc. www.earthsearch.com, HyVista, www.hyvista.com).

The same methodology used by exploration professionals can be certainly used by environmentalists for the detection of oil-contaminated sites, indicative of environment-threatening oil spilling and leakage.

Examples of airborne hyperspectral data applied for oil spills detection are available.

The Probe-1 data, integrated with field and subsurface geological and geochemical data, have been used to predict possible sites of hydrocarbon microseepage in the Ventura Basin (Santa Barbara), in Southern California (van der Meer et al. 2002). The AISA sensor has been used to monitor the Chesapeake Bay, where major interstate commerce routes, underground pipelines, extensive development, large industrial facilities and heavy shipping traffic to the port of Norfolk and Baltimore exist, and which suffered during the last several decades of several large spill events threatening coastal habitats and species (Sanchez et al. 2003, Salem et al. 2005). Hyperspectral AVIRIS data have been used for oil spill detection and oil spill type classification, using advanced techniques, in the Santa Barbara County (Salem and Kafatos, 2004). The HyMap sensor has been successfully used to detect and measure chemical and physiographic variability within the hydrocarbon seepage off Coal Oil Point, Santa Barbara, CA: one of the largest and most active seeps in the world (HyVista Corporation, 2006).

The open challenge for the future of hyperspectral remote sensing of oil-impacted sites is the shift to satellite monitoring. This will allow exploiting all the advantages that satellites provide: synoptic view, global coverage, high repetitive acquisition and low data cost.

It is finally worthwhile to list some other potential applications of hyperspectral remote sensing for marine and maritime surveillance.

Airborne hyperspectral remote sensing has already been used to gather qualitative and quantitative information on seafloor in clear shallow waters (Louchard et al. 2002). Results indicate that derivative analysis of hyperspectral remote sensing data is a potentially powerful method for detailed analysis of benthic substrates. Since the hydrocarbon absorption peaks belong to an EM region (the SWIR) where water is so absorbent that, even in shallow waters, no seafloor signal is detectable, this methodology could not be used to unambiguously detect hydrocarbon sediments on the seafloor. Nevertheless the

methodology could be used to monitor changes in the benthic substrate, which could give indirect evidence of oil-sedimentation.

Hyperspectral imagery may offer the potential to unambiguously identify the hold material released by ships (i.e., ballast water, dredged sediment dumping, sewage and trash dumping). As an example, Fig. 9 shows a HyMap sensor image detecting a ship caught in the process of emptying its hold (source: www.HyVista.com). Recently, SeaWiFS data have been used to individuate the cell concentration in zone of ballast water exchange.
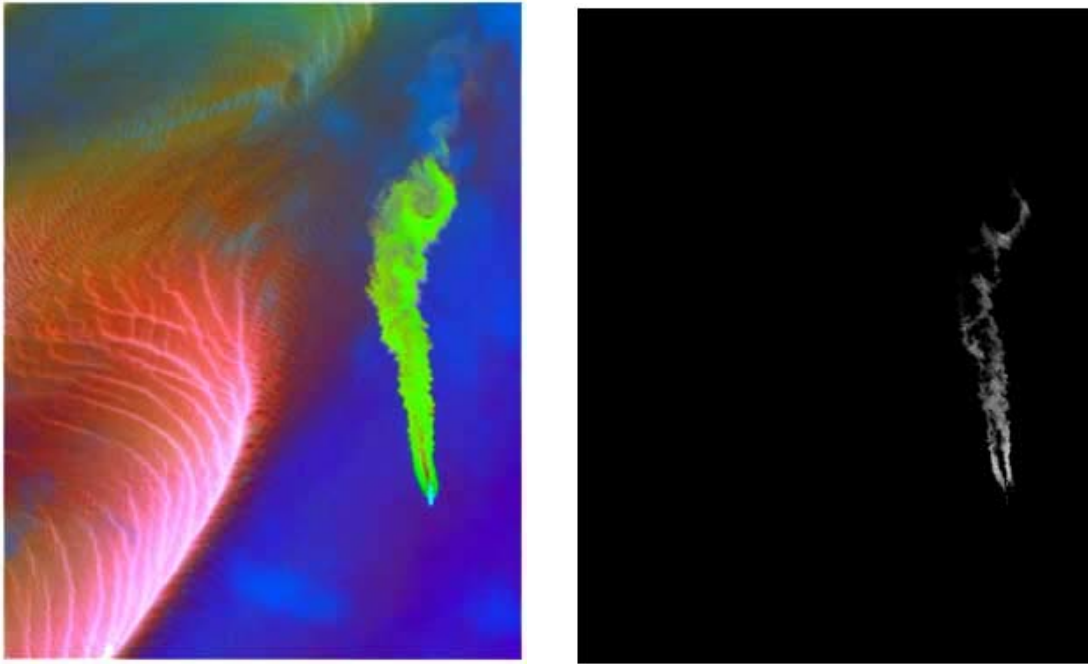

Image courtesy of HyVista Corporation.

Figure 9. HyMap image acquired on the 9th Nov, 1998 at Moreton Bay, Queensland Coast, Australia. The sandy bottom can clearly been seen in this shallow water image to the left, while the ship seen on the right was caught in the process of emptying its hold. Simple spectral processing leveraging the many bands of HyMap allows for unique identification of hold material.

Finally, hyperspectral data could be usefully applied in monitoring the effects on aquatic ecosystems of non-indigenous species. These are increasingly conspicuous in marine and estuarine environments throughout the world, and their invasions are linked to ballast water. Invasive aquatic species are one of the greatest threats to the world's oceans, and can cause extremely severe environmental, economic and public health impacts.

5. Toward an oil dedicated spectral library: laboratory and *in situ* measurement of the spectral signature of oil and oil-impacted soil

As pointed out in the previous Section 3, a fundamental step in the correct interpretation of hyperspectral data is the availability of dedicated spectral libraries. Libraries are built measuring in the laboratory and cataloging the spectral signatures of the target elements. A major challenge indeed, since a large *in situ* database needs to be acquired.

In this Section, the spectral measurements performed both in laboratory and *in situ* will be described.

5.1 Description of the Measurements

A Perkin Elmer Lambda 19 double-beam spectrophotometer (Fig.10) equipped with a $BaSo_4$ integrating sphere was used for the measurements of the reflectance of the oil-impacted soil samples.

Spectra were scanned over the 400-2500 nm wavelength interval with 1 nm step starting at 2500 nm and ending at 400 nm. The spectral resolution varied from 1 to 2 nm in the visible/ near infrared (400-1000nm) and from 4 to 5 nm in the middle infrared (1000-2500 nm).

The calibration of the instrument was performed using Spectralon^{TM} reflectance and wavelength calibration standards. For each sample, five different spectrometric measurements were made.
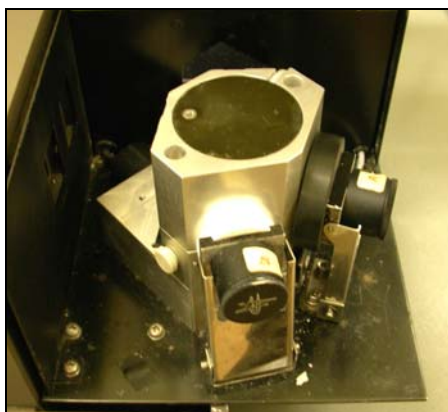

Fig: 10 Spectrophotometer in Reflectance mode

An additional series of measurements was performed on samples of the oil spilt from the Erika and the Prestige tankers during the major accidents of 1999 and 2002. A portable high resolution spectroradiometer ASD-FieldSpec Pro (Analytical Spectral Devices) (Fig. 11), suitable for *in situ* measurements, was used in the 350-2500 nm range.

Fig.11 The spectroradiometer ASD-FieldSpec Pro in Reflectance mode

5.2. Preparation of the oil-contaminated soil samples

The samples of oil-contaminated soils were prepared by making use of pure sand (fig. 12) and a loamy type soil composed of 78% sand, 20% silt and 2% clay (fig. 13). Soil samples were put in black PVC supports and heated in an oven at 110°C for 48 hours to remove any residual humidity.

Only a few minutes before the spectral measurements, some drops of hydrocarbons were added to the samples. Four different types of hydrocarbons were used: those more commonly discharged by ships and, for their longer evaporation time, those having a permanence on water and soil: diesel oil, used oil, and two types of crude oil: "Es Sider" light crude oil and "Iranian Heavy" heavy crude oil.

The "Es Sider" oil has been obtained from the Tamoil refinery in Cremona, Italy; the "Iranian Heavy" from the IES refinery in Mantova, Italy; the other hydrocarbons are those commonly found in commerce. In addition, samples of the oil spilt from the Erica tanker during the accident which occurred in December 1999 off the west coast of France and from the Prestige tanker during the accident which occurred in November 2002 off the north-west coast of Spain, were obtained at the sites, and analyzed in their pure state.

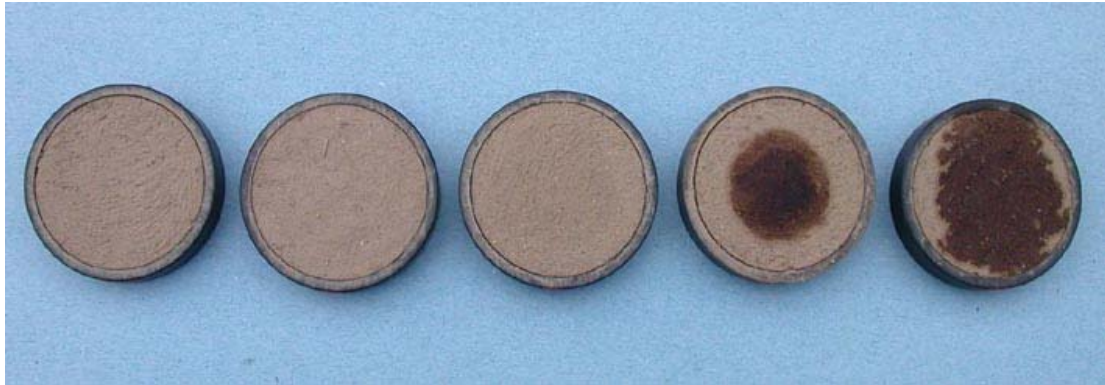*Fig: 12 Samples of pure sand and oil-impacted sand.*

Fig:13   Samples of pure soil and oil-impacted soil

5.3. Analysis of the results

As already demonstrated by Cloutis (1989), the hydrocarbon-bearing reference objects are characterized by absorption maxima at wavelengths 1730 and 2310 nm.

These absorption peaks are typical of the C-H stretch: in particular, 1730 nm is the C-H Stretch 1st Overtone band, and 2310 nm is the C-H stretch Combination band.

Fig. 14 shows the reflectance spectrum of pure sand and sand samples contaminated by diesel oil, used oil, "Es Sider" and "Iranian Heavy" crude oils. The two typical hydrocarbons peaks are clearly visible in the oil-impacted samples.
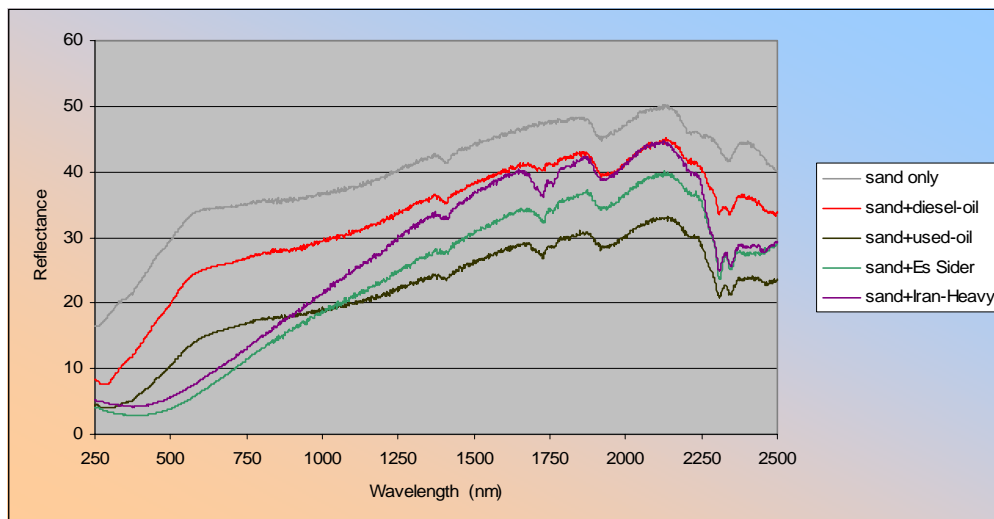

Fig 14: Spectral signatures of pure sand and oil-impacted sand

Fig. 15 shows an analogous plot for samples of oil-impacted soil. Also in this case, the two peaks at 1730 and 2310 nm are visible, with particular evidence for crude oil contamination.
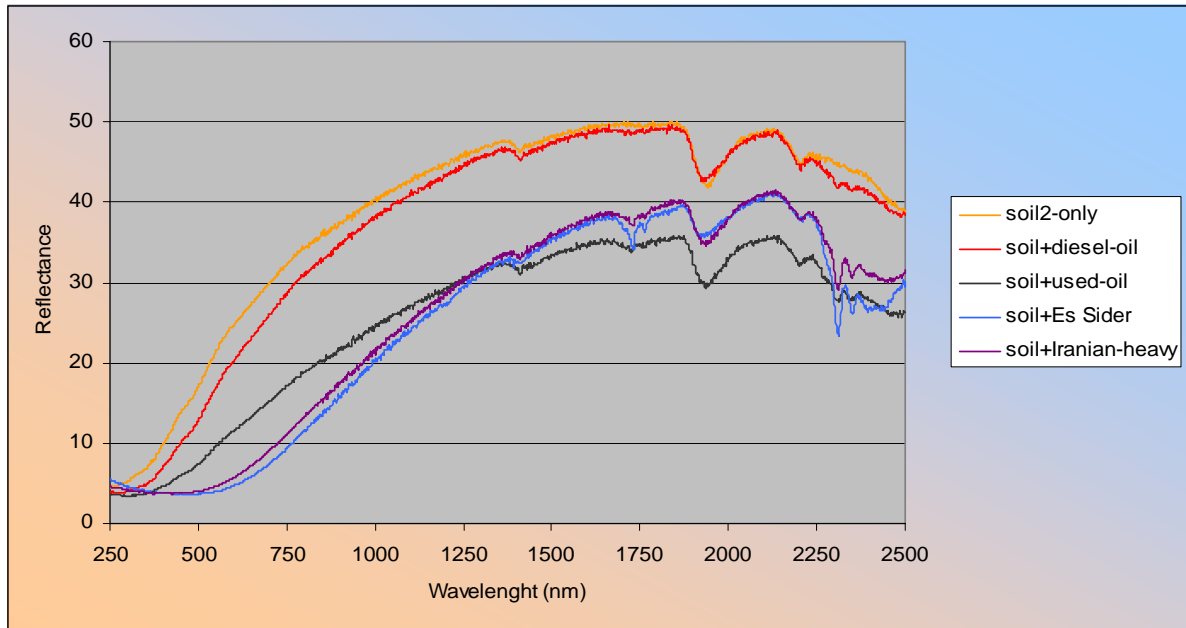

Fig 15: Spectral signatures of pure soil and oil-impacted soil

Finally, figure 16 shows the reflectance spectra of the samples of the oils spilt from the Erika and Prestige tankers. They were analyzed with the portable Spectroradiometer ASD-Field Spec, in reflectance mode. For both oils, the two C-H stretch absorption peaks are clearly visible.
Cloutis (1989) and afterwards Hoerig et al. (2001) found that the strength of the signal is proportional to the oil content.

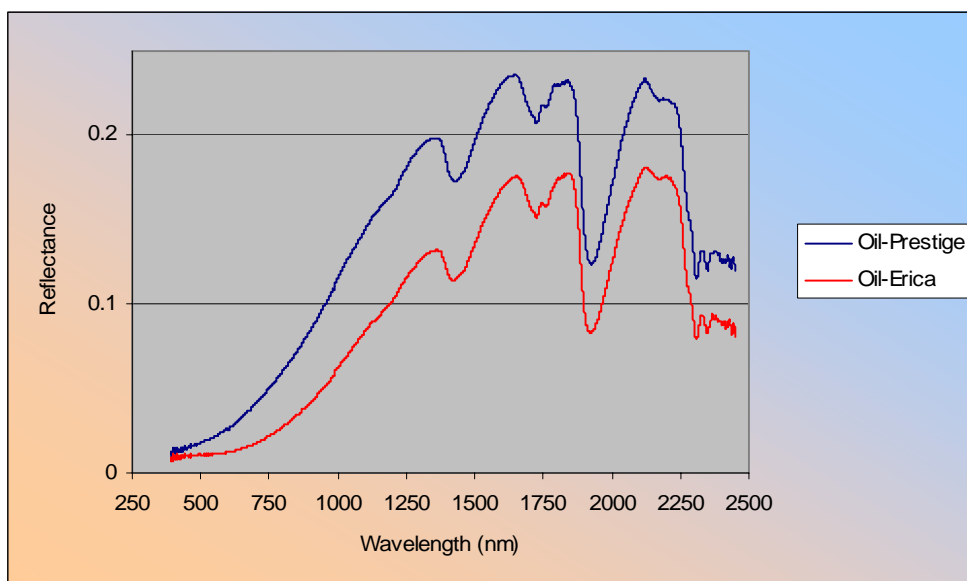*Fig.16 Spectral signature of the oil spilt from the Prestige and Erika tankers*

Additional experimental tests have been performed to analyze the consistency of the signal when the sample is put under ordinary meteorological conditions. Successive measurements made months or even years after sample collection and preparation showed unchanged results. This strengthens the validity of the test.

6. Summary and conclusions

Hyperspectral remote sensing shows great potentialities in the monitoring of oil spills in the marine environment.

Hyperspectral data are not all-weather all-day available, but they have the ability to measure an intrinsic property of the oil: its spectral signature. As a consequence, hyperspectral sensors offer the potential to unambiguously detect oil features, distinguish between oil types (crude/light oil), give indication on oil slick thickness and even detect submerged oil and emulsions.

While several different airborne hyperspectral sensors exist, only two technology demonstrator satellite hyperspectral sensors are nowadays available. Others are foreseen in the near future.

Airborne hyperspectral remote sensing is routinely used to detect natural oil seeps, as indicator of potential petroleum accumulation.

The same methodologies developed for exploratory purpose can certainly be extended to monitor oil pollution threatening the environment.

A correct interpretation of hyperspectral data generally requires a pre-processing stage to remove the atmospheric noise (which can be consistent for marine data); the extraction of endmembers spectral signature and their identification via spectral library match.

Spectral libraries are a collection of the spectral signatures of the target materials. They require the *in situ* collection and laboratory spectroscopic analysis of the investigated samples.

For oil pollution monitoring purpose, an oil dedicated spectral library is needed, including the spectral signature of oil and oil-impacted soils.

To this aim, laboratory analysis have been performed in the frame of the MDIV project, over samples of oil-impacted soils and of crude oil spilled during the Erica and Prestige tank disaster.

At present no operational use of hyperspectral satellite sensors for oil spill monitoring is possible, but the future of hyperspectral remote sensing in this field is highly promising.

7. Bibliography

Adams, J. B., Smith, M. O., and Johnson, P.E., Spectral mixture modeling: A new analysis of rock and soil types at the Viking Lander 1 site. Journal of Geophysical Research, vol. 91(B8), pp. 8090-8112. (1986)

Andreoli G., P. Viaud, B. Hosgood, "Hyperspectral Characterization of Soil Types applied to Demining", *JRC Ispra, S.P.I.03.16 (2003)*

Blackburn, G. A.. "Quantifying chlorophylls and carotenoids at leaf can canopy scales: an evaluation of some hyperspectral approaches". Remote Sensing Reviews, 66:273– 285. (1998)

Boardman, J.W.,"Inversion of imaging spectrometry data using singular value decomposition". *Proc. of the Twelfth Canadian Symposium on Remote Sensing*, v. 4, pp. 2069-2072. (1989)

Boardman, J. W., "Automated spectral unmixing of AVIRIS data using convex geometry concepts: in Summaries", *Fourth JPL Airborne Geoscience Workshop*, JPL Publication 93-26, 1:11-14. (1993)

Boardman, J. W., F. A. Kruse and R.O. Green,"Mapping target signatures via partial unmixing of AVIRIS data: in Summaries", *Fifth JPL Airborne Earth Science Workshop*, JPL Publication 95-1, 1:23-26. (1995)

Brekke C., and A.H.S. Solberg, "Oils spill detection by satellite remote sensing", Remote Sensing of Environment, 95, 1-13, (2005)

Bulgarelli B. and D. Tarchi, "Exploratory use of MODIS in oil spill monitoring", in Workshop on Monitoring Activities Related to the Oil Pollution in Lebanon ed., G. Ferraro, D. Tarchi, G. L. Ruzzante, A. Sieber, EUR 22531

Byfeld V. and S. Boxal, "Thickness estimated and classification of surface oil using passive sensing at visible and near-infrared wavelength", in *Proc. Of the IEEE International Geoscience and Remote Sensing Symposium* (1999)

Cairns B., B. E. Carlson, R. Ying, A.A. Lacis and V. Oinas, "Atmospheric Correction and Its Application to an Analysis of Hyperion Data", IEEE Transaction on Geoscience and Remote Sensing, vol. 41, no. 6, (2003)

Clark, R.N. and Swayze, G.A.. "Mapping minerals, amorphous materials, environmental materials, vegetation, water, ice and snow, and other materials: The USGS Tricorder Algorithm". *Summaries of the Fifth Annual JPL Airborne Earth Science Workshop*, January 23- 26, R.O. Green, Ed., JPL Publication 95-1, p. 39-40. (1995)

Clark, R.N., Swayze, G.A. Livo, K.E. Kokaly, R.F. Sutley, S.J. Dalton, J.B. McDougal, R.R. and Gent, C.A.. "Imaging Spectroscopy: earth and planetary remote sensing with the USGS Tetracorder and expert systems", Journal of Geophys Research, 18(E12):5131. (2003)

Cloutis E. "Spectral Reflectance Properties of Hydrocarbons: Remote-Sensing Implications", Science, 245, 165-168, (1989)

David L.B. Jupp, "Discussion around Hyperion Data", CSIRO Office of Space Science & Applications Earth Observation Centre, http://www.eoc.csiro.au/hswww/oz_pi/docs/Hyp_Notes.pdf, accessed on November the 10th 2006,

Ellis JM, HH Davis, JA Zamudio, "Exploring for onshore oil seeps with hyperspectral imaging", Oil and gas Journal, vol. 99.37, p. 49-58 (2001)

Ellis JM, "Hyperspectral imaging technologies key for oil seep/oil-impacted soil detection and environmental baselins", Environmental Science and Engineering. Retrieved on Feb. 23, 2004 from http://www.esemag.com/0503/index.html (2003)

Fingas M. and C.E. Brown, "Review of oil spill remote sensing", Spill Science and technology Bulletin, 4, 199-208 (1997)

Gao B.- C., K.B. Heidebrecht and A.F.H. Goetz, *Atmosphere Removal Program (ATREM) Version 2.0 Users Guide,* Center for the Study of Earth from Space/CIRES, University of Colorado, Boulder, Colorado, **26 (**1996).

Gao B.-C., M.J. Montes, Z. Ahmad and C.O, Davis, "Atmospheric correction algorithm for hyperspectral remote sensing of ocean color from space", Applied Optics, vol. 39, no. 6, pg. 887-896, (2000)

Green R.,"Atmospheric Correction Now (ACORN),*"* developed by ImSpec LLC, available from Analytical Imaging and Geophysics LLC, (2001).

Gruninger J., R.L. Sundberg, M.J. Fox, R. Levine, W.F. Mudkowsky, M.S. Salisbury and A.H. Ratcliff,"Automated Optimal Channel Selection for Spectral Imaging Sensors", *Proc. SPIE 4381, Algorithms for Multispectral and Hyperspectral Imagery VII,* 4381-07 (2001)

Hoerig B., Kuehn F., F. Oschuetz and F. Lehmann, "HyMap hyperspectral remote sensing to detect hydrocarbons", Int. J. Remote Sensing, vol. 22, no. 8, 1413-1422 (2001)

Hosgood B., G. Andreoli. Laboratory measurements of spectral signatures of marine pollutants. *JRC Ispra EUR 19019 EN* (1999)

Hu C., F.E. Mueller-Krager, C. Taylor, D. Myhre, B. Murch, A.L. Odriozola and G. Godoy, "MODIS detects oil spill in Lake Maracaibo, Venezuela", EOS Vol. 84, n. 33. (2003)

HyVista Corporation, "Mapping Natural Hydrocarbon Seeps. Santa Barbara, California, USA", accessed from www.Hyvista.com on November 2006.

Kuehn F. and B. Heorig, "Environmental Remote Sensing of Military Exercise Areas in Germany", Remote Sensing and GIS for site characterization: Applications ad Standards, ASTM STP 1279, V.H. Singhroy, D.D. Nebert and A.I. Johnoson Eds., American Society for testing Materials, pp. 107-116 (1995)

Kuehn F., K. Oppermann and B. Hoerig, "Hydrocarbon Index – an algorithm for hyperspectral detection of hydrocarbons", Int. J. Remote Sensing, vol. 25, 12, 2467-2473, (2004)

Kruse F.A., A.B. Letkoff, J.W. Boardman, K.B. Heidebrecht, A.T. Shapiro, P.J. Barloon and A.F.H. Goetz,"The Spectral Image Processing System (SIPS) – interactive visualization and analysis of imaging spectrometer data", Remote Sensing of Enviroment, 44, 145-163 (1993)

Liang S. and H. Fang, "An Improved Atmospheric Correction Algorithm for Hyperspectral Remotely sensed Imagery", IEEE Geosc. and Rem. Sens., 1 (2), 112-117 (2004)

Louchard E. M., R.P. Reid, C.F. Stephens, C.O. Davis, R.A. Leathers, T.V. Downes, R. Maffione, "Derivative analysis of absorption features in hyperspectral remote sensing data of carbonate sediments", Optics Express, vol. 10, n. 26, 1573-1584 (2002)

Matthew M.W., S.M. Adler-Golden, A. Berk, S.C. Richtsmeier, R.Y. Levine, L.S. Bernstein, P.K. Acharya, G.P.Anderson, G.W. Felde, M.P. Hoke, A. Ratkowski, H.-H. Burke, R.D. Kaiser, and D.P. Miller, *"Status of Atmospheric Correction Using a MODTRAN4-based Algorithm," SPIE Proceeding, Algorithms for Multispectral, Hyperspectral, and Ultraspectral Imagery VI*, **4049**, pp. 199-207, (2000).

NASA, "Remote Sensing Tutorial". Principal Author: Nicholas M. Short, NASA Official: J. Bolton, Website Curator: Laura Rocchio, site last update May 19, 2006. http://rst.gsfc.nasa.gov

NRC (National Research Council) Committee on Oil in the Sea: Inputs, Fates, and Effects,"Oil in the sea III: Inputs, fates and effects", Report 2003. U.S. National Academy of Sciences.

Otremba Z. and J. Piskozub, "Modeling the optical contrast of an oil on a sea surface, Optics Express, 9 (8), 411-416 (2001)

Otremba Z. and J. Piskozub, "Modeling the remotely sensed optical contrast caused by oil suspended in the sea water column", Optics Express, 11 (1), 2-6 (2002)

Otremba Z. and J. Piskozub, "Modeling the bidirectional reflectance distribution function (BRDF) of sweater polluted by an oil film", Optics Express, 12 (8), 1671-1676 (2004)

Phinney J.T., F. Muller-Karger, P. Dustan, J. Sobel, "Using Remote Sensing to Reassess the Mass Mortality of Diadema antillarum 1983-1984", Conservation Biology ,Vol. 15 Issue 4 Page 885, August (2001)

Qu Z., Kindel B.C., Goetz A.F.H.,"The (HATCH) model : Earth Observing 1 mission". IEEE transactions on Geoscience and Remote Sensing , vol. 41 (1), n°6, pp. 1223-1231 (2003)

Richards, J.A., and Jia, X., "Remote Sensing Digital Image Analysis, an Introduction". Fourth Edition. Springer-Verlag: Berlin (2006).

Richter R., *"Correction of atmospheric and topographic effects for high spatial resolution satellite imagery"*, Int. J. Remote Sensing **18**:1099-1111, 1997.

Salem F., M. Kafatos, T. El-Ghazawi, R. Gomez and R Yang, "Hyperspectral image assessment of oil-contaminated wetland", Int. J. of Remote Sensing, vol. 26, n.4, 811-821 (2005)

Salem, F., and Kafatos, M., "Hyperspectral Partial Unmixing Technique for Oil Spill Target Identification," XX th Congress International Society for Photogrammetry and Remote Sensing", Conference 21-23 July 2004, Istanbul, Turkey (2004).

Sanchez G, W.E. Roper, R. Gomez, "Detcetion and Monitorino of Oil Spills using Hyperspectral Imagery", *Geo-Spatial and Temporal Image and data Exploration III, Nickolas L. Faust, W.E. Ropers, Editors,* Proc. of SPIE, vol. 5097, 233-240, (2003)

Shippert P., " Why Use Hyperspectral Imagery?", Photogrammetric Engineering & Remote Sensing Journal of the American Society for Photogrammetry and Remote Sensing, volume 70, number 4 (2004)

Tsai F, and W. Philpot,"Derivative analysis of Hyperspectral data", Remote Sens. Environ., 66, 41-51 (1998)

van der Meer F., P. van Dijk, H. van der Werff and H. Yang. Remote sensing and petroleum seepage:a review and case study. *International Institute for Aerospace Survey and Earth Sciences ITC, Division of Geological Survey, Enschede, Netherlands. (Blackwell Science Ltd. 2002)*
X. Liu, W. L. Smith

Abstract

While conventional multispectral sensors record the radiometric signal only at a handful of wavelengths, hyperspectral sensors measure the reflected solar signal at hundreds contiguous and narrow wavelength bands, spanning from the visible to the infrared. Hyperspectral images provide ample spectral information to identify and distinguish between spectrally similar (but unique) materials, providing the ability to make proper distinctions among materials with only subtle signature differences. Hyperspectral images show hence potentiality for proper discrimination between oil slicks and other natural phenomena (look-alike); and even for proper distinctions between oil types. Additionally they can give indications on oil volume.

At present, many airborne hyperspectral sensors are available to collect data, but only two civil spaceborn hyperspectral sensors exist as technology demonstrator: the Hyperion sensor on NASA's EO-1 satellite and the CHRIS sensor on the European Space Agency's PROBA satellite. Consequently, the concrete opportunity to use spaceborn hyperspectral remote sensing for operational oil spill monitoring is yet not available. Nevertheless, it is clear that the future of satellite hyperspectral remote sensing of oil pollution in the marine/coastal environment is very promising.

In order to correctly interpret the hyperspectral data, the retrieved spectral signatures must be correlated to specific materials. Therefore specific spectral libraries, containing the spectral signature of the materials to be detected, must be built up. This requires that highly accurate reflected light measurements of samples of the investigated material must be performed in the lab or in the field.

Accurate measurements of the spectral reflectance of several samples of oil-contaminated soils have been performed in the laboratory, in the 400-2500 nm wavelength range. Samples of the oils spilt from the Erika and the Prestige tankers during the major accidents of 1999 and 2002 were also collected and analyzed in the same spectral range, using a portable spectrophotometer. All measurements showed the typical absorption features of hydrocarbon-bearing substances: the two absorption peaks centered at 1732 and 2310 nm.

EUROPEAN COMMISSION
DIRECTORATE-GENERAL
Joint Research Centre

Mission of the JRC

The mission of the JRC is to provide customer-driven scientific and technical support for the conception, development, implementation and monitoring of EU policies. As a service of the European Commission, the JRC functions as a reference centre of science and technology for the Union. Close to the policy-making process, it serves the common interest of the Member States, while being independent of special interests, whether private or national.

Publications Office
Publications.eu.int

Hyperspectral Analysis of Oil and Oil-Impacted Soils
for Remote Sensing Purposes

EUR 22739 EN